Ground state structure of diluted antiferromagnets and random field systems

Alexander K. Hartmann
Institut für theoretische Physik, Philosophenweg 19,
69120 Heidelberg, Germany
Tel. +49-6221-549449, Fax. +49-6221-549331
hartmann@tphys.uni-heidelberg.de*
and
Theoretische Tieftemperaturphysik, Gerhard Mercator Universität,
47048 Duisburg, Germany

A method is presented for the calculation of all exact ground states of diluted Ising antiferromagnets and random field Ising systems in an arbitrary range of magnetic fields $B \in [B_{start}, B_{end}]$ resp. $\Delta \in [\Delta_{start}, \Delta_{end}]$. It works by calculating all *jump*-fields B, Δ where the system changes it's ground state. For each field value all degenerated ground states are represented by a set of (anti-) ferromagnetic clusters and a relation between the clusters. So a complete description of the ground state structure of these systems is possible.
Systems are investigated up to size 48^3 on the whole field-range and up to 160^3 for some particular fields. The behavior of order parameters is investigated, the number of jumps is analyzed and the degree of degeneracy as functions of size and fields is calculated.
Keywords (PACS-codes): random systems (75.10.N), ground state calculation (75.40.H), order parameters (75.40.C), graph theory (02.10).

I. INTRODUCTION

The behavior of diluted Ising antiferromagnets in a homogeneous field (DAFF) and of random field Ising ferromagnets (RFIM) is still not well understood (for a review see [1]). Although it has been argued that DAFF and RFIM belong to the same universality classes [2,3] recent results [4–7] suggest that there might be essential differences.
In [8] integer optimization algorithms where applied to the RFIM in order to calculate exact ground states at fixed fields in polynomial time. In [9] different degenerated ground states of DAFFs and RFIMs were calculated by using a simple extension of these optimization methods.
The invention of new fast algorithms [10] inspired us to develop an algorithm which calculates the ground states for all fields and is presented in this paper. Additionally the complete degenerated structure of a ground state is computable at once, by the use of some more complex algorithms from graph theory [11] . Applying these methods a far better insight into the nature of ground states of disordered systems is possible.
All systems we investigated were cubic $LxLxL$ lattices of Ising spins $\sigma_i = \pm 1$ with periodic boundary conditions. For a DAFF each lattice site is occupied ($\epsilon_i = 1$) with probability p (otherwise $\epsilon_i = 0$). The DAFF is described by the following Hamiltonian

$$H = J \sum_{<i,j>} \epsilon_i \epsilon_j \sigma_i \sigma_j - B \sum_i \epsilon_i \sigma_i \tag{1}$$

with the uniform external field $B > 0$ and the interaction constant $J > 0$. The sum $< i, j >$ runs over all pairs of nearest neighbors. For low temperatures and small fields $B < B_c$ the DAFF has an antiferromagnetic phase. In this paper we show for the critical field $B_c \approx 0.9$. For finite fields and low temperatures exists a frozen domain state which is characterized by fractal domains [5,7,12]. For higher fields or higher temperatures the DAFF is paramagnetic.
The Hamiltonian for the RFIM is

$$H = -J \sum_{<i,j>} \sigma_i \sigma_j - \sum_i B_i \sigma_i \tag{2}$$

All sites ore occupied, but the magnetic fields B_i are site dependent and distributed according a bimodal ($\pm\Delta$-RFIM) or a Gaussian (Gaussian-RFIM) probability distribution. Their probability density functions are

$$p(B_i) = \frac{1}{\sqrt{2\pi}\Delta} e^{-(B_i/\sqrt{2}\Delta)^2} \tag{3}$$

$$p(B_i) = \frac{1}{2}(\delta(B_i - \Delta) + \delta(B_i + \Delta)) \tag{4}$$

Like the DAFF the 3d RFIM has a long range ordered low temperature and low field phase, a disordered phase for finite fields (critical field: $\Delta_c = 2.35$ [8]) and is paramagnetic for high temperatures or high fields.
The outline of the paper is as follows. The first section explains how all degenerated ground states of a system at a fixed field value can be represented by a relation of clusters. The second section gives an algorithm which calculates

*permanent address

the ground states for all fields. In the third section we show the results of our calculations. We present the order parameter for sample systems of different sizes, estimate the values for the critical fields, analyze how the number of jumps increases with increasing system size and investigate the degree of degeneracy as function of field and size. In the last section we summarize our results.

II. CALCULATION OF A GROUND STATE

We used well known algorithms from graph theory [13–15] to calculate the ground state of a system at given field B, Δ and interaction constant J. All quantities B, Δ, J have to be integer-valued. The calculation works by transforming the system into a network [16], and calculating the maximum flow [10,17]. [1] All degenerated ground states of the system are given [11] by a set $\overline{V} = \{S = V_0, V_1, \ldots, V_n, V_{n+1} = T\}$ of clusters, and a binary relation $\overline{R}$ defined on $\overline{V}$. Each cluster V_i is a set of antiferromegnetically (DAFF) resp. ferromagnetically (RFIM) ordered spins. These spins are not necessarily spatial connected.
From the pair $(\overline{V}, \overline{R})$ a ground state is calculated in the following way. Each cluster V_k $(k = 0, \ldots, n+1)$ is assigned a *orientation* (or *sign*) $s(V_k)$:
The signs of the clusters S, T are determined: $s(S) = 1$, $s(T) = -1$. For all other clusters V_k $(k = 1, \ldots, n)$, called *inner clusters*, the sign can be chosen free $(s(V_k) = \pm 1)$ under consideration of the condition $(l = 1, \ldots, n)$:

$$\text{if } (s(V_k) = +1 \text{ and } (V_k, V_l) \in \overline{R}) \text{ then } s(V_l) = +1 \tag{5}$$

I.e., if a cluster has the sign $+1$, then all successors in the relation $\overline{R}$ must have the sign $+1$ too.
From the signs of the clusters the spin states of the spins $i \in V_k$ are calculated by

$$\sigma_i = t(i)s(V_k)(\text{DAFF}) \tag{6}$$
$$\sigma_i = \quad s(V_k) \quad (\text{RFIM}) \tag{7}$$

The function $t(i)$ divides the lattice of the DAFF into two sublattices: $t(i) = (-1)^{x+y+z}$ for a spin i with coordinates (x, y, z). So the clusters S, T consist of the spins with fixed states, for each direction one cluster, all other clusters contain spins which contribute to the degeneracy of the ground state. The dependencies between spins of adjacent clusters are given by the relation $\overline{R}$
As example we consider an one dimensional RFIM chain with open ends consisting of four spins $\sigma_1, \ldots, \sigma_4$. The random fields are $B_1 = 2, B_2 = B_3 = 0, B_4 = -2$ $(J = 1)$. So the states of the end-spins are fixed in the ground state $\sigma_1 = 1, \sigma_4 = -1$. The states of the inner spins are not fixed. The system is visualized in figure 1.

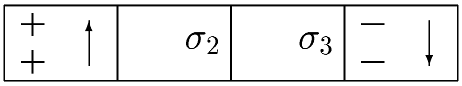

FIG. 1. Example RFIM system with four spins.

The energy of the system as function of the two inner spins is $H = -4 - \sigma_2 + \sigma_3 - \sigma_2\sigma_3$. The energies for the four possible states are shown in the table in figure II.

σ_2	σ_3	H
$+1$	$+1$	-5
$+1$	-1	-5
-1	$+1$	-1
-1	-1	-5

FIG. 2. Ground state energies for sample system.

So the ground state of the system is threefold degenerated. It can be described by the rule: The inner spins are not fixed, but if $\sigma_3 = +1$ then $\sigma_2 = +1$ must hold too. So the ground state is formally given by

$$\overline{V} = \{S, V_1, V_2, T\}, S = \{1\}, V_1 = \{2\}, V_2 = \{3\}, T = \{4\} \tag{8}$$

and

$$\overline{R} = \{(2, 1)\} \tag{9}$$

[1]Implementation details: We used Tarjan's wave algorithm together with the heuristic speed-ups of Träff. In the construction of the *level graph* we allowed not only edges (v, w) with level(w) = level(v)+1, but also all edges (v, t) where t is the sink. For this measure, we observed an additional speed-up of roughly factor 2 for the systems we calculated.

The ground state can be displayed as a graph. The nodes represent the clusters and the edges represent the relation. Because for 'real' systems the clusters are too large, only the order parameter of each cluster is given in the graph, instead of enumerating all spins. For the inner clusters, where the order parameter can take two values, the value for the cluster orientation $s(V_k) = -1$ is displayed. So the example system is represented by the graph shown in figure 3.

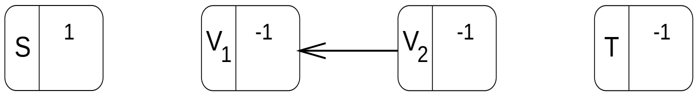

FIG. 3. Ground state of example RFIM given by the relation $\overline{R}$.

III. CALCULATION OF GROUND STATES FOR ALL B, Δ

Let's examine a Cluster C in a DAFF with magnetization $m_C = m_C^{\uparrow} - m_C^{\downarrow}$ ($m_C^{\uparrow}, m_C^{\downarrow} \geq 0$ denote the number of spins in up and down direction). The cluster is supposed to exist as a coherent unit for an finite B-interval $[B_1, B_2]$. Without loss of generality all other clusters can be supposed to keep their orientations inside this interval.
The cluster is connected to its environment by N_C^s satisfied and N_C^u unsatisfied bonds. The part of the cluster energy describing its connection to its surface and to the external field is

$$E_c(B) = (N_C^u - N_C^s)J - m_C B = (N_C^u - N_C^s)J - (m_C^{\uparrow} - m_C^{\downarrow})B \tag{10}$$

($N_C^u, N_C^s, m_C^{\uparrow}, m_C^{\downarrow}$ depend itself on B.) For a ground state $E_c(B) \to \min$ holds. Let's suppose that the cluster flips its orientation at $B = B^j \in [B_1, B_2]$. That implies that the magnetization of the cluster is nonzero, because the environment of the cluster is supposed to be unchanged, and otherwise there would not occur a jump. Since the number of satisfied/unsatisfied bonds and the number of up/down spins exchange, when a cluster is flipped, the energy of a flipped cluster changes its sign. That implies $E_c(B^j) = 0$, because $E_c(B) \leq 0$ for all $B \in [B_1, B_2]$. So the cluster can take both orientations at $B = B^j$. That leads to

$$B^j/J = \frac{N_C^u - N_C^s}{m_C^{\uparrow} - m_C^{\downarrow}} \tag{11}$$

($N_C^u, N_C^s, m_C^{\uparrow}, m_C^{\downarrow}$ all from $B < B^j$ or all from $B > B^j$.) Because the cluster C is part of cluster S or T, these values are not directly accessible, we want to express this "jump-field" B^j using characteristic values of the graphs $\overline{R}$ immediately "before" ($B < B^j$) and "after" ($B > B^j$) the jump. Because the cluster does not contribute to the degeneracy (which holds only for clusters with zero magnetization and $N_C^u = N_C^s$) it moves during the jump from the (super)cluster S to T or vice versa. So we get (m_S, m_T: magnetizations of S, T)

$$|m_C^{\uparrow} - m_C^{\downarrow}| = |m_T(B < B^j) - m_T(B > B^j)| \quad \left(= |m_S(B < B^j) - m_S(B > B^j)|\right) \tag{12}$$

Using $N_C^u(B < B^j) - N_C^s(B < B^j) = N_C^u(B < B^j) - N_C^u(B > B^j) = N^u(B < B^j) - N^u(B > B^j)$ (the rest of the system does not change, N^u = total number of unsatisfied bonds in the system) and because $B^j/J > 0$ we have as result:

$$B^j/J = \frac{|N^u(B < B^j) - N^u(B > B^j)|}{|m_T(B < B^j) - m_T(B > B^j)|} \tag{13}$$

For a RFIM the formula describing the relevant terms of the energy of a cluster (similar to (10)) is

$$E_c(\{B_i\}) = (N_C^u - N_C^s)J - \sum_{i \in C} B_i \sigma_i \tag{14}$$

A given realization of a RFIM is determined by the local field values $b_i := B_i(\Delta = 1)$, so $B_i = \Delta b_i$. For the $\pm\Delta$-RFIM the b_i is just the *sign* of the random field. Defining the total random field sign of the cluster by $\Sigma_C := \sum_{i \in C} b_i$ we get

$$E_c(\Delta) = (N_C^u - N_C^s)J - \Sigma_C s(C)\Delta \tag{15}$$

Comparing with (10) we see that $\Sigma_C s(C)$ plays the role of the magnetization and Δ is equivalent to the external field B of a DAFF. A RFIM cluster moves at a jump from the super-cluster S to T or vice versa, so we have $|\Sigma_C| = |\Sigma_T(\Delta < \Delta^j) - \Sigma_T(\Delta > \Delta^j)|$ and $|s(C)| = 1$. So the field Δ^j where the cluster flips is calculated by:

$$\Delta^j/J = \frac{|N^u(\Delta < \Delta^j) - N^u(\Delta > \Delta^j)|}{|\Sigma_T(\Delta < \Delta^j) - \Sigma_T(\Delta > \Delta^j)|} \tag{16}$$

For illustration in Figures 4 to 6 the ground states of a sample DAFF system ($L = 10$, $p = 0.5$) are displayed for $9/7 < B < 1.6$. In addition to the order parameter of each cluster (upper value) its magnetization (lower value) is given.

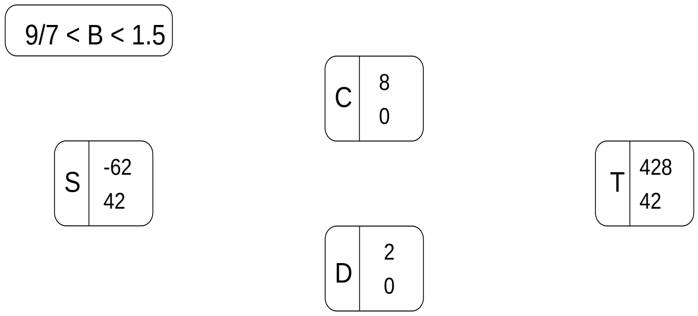

FIG. 4. Ground state $\overline{R}$ of sample DAFF ($L = 10$, $p = 0.5$) for $9/7 < B < 1.5$.

A cluster with zero magnetization and equal number of satisfied and unsatisfied bonds can take both orientations over a range of external fields. For $9/7 < B < 1.5$ these holds for clusters C, D. The degeneracy of the system has degree $2x2 = 4$, because each cluster C, D can take independently two orientations.

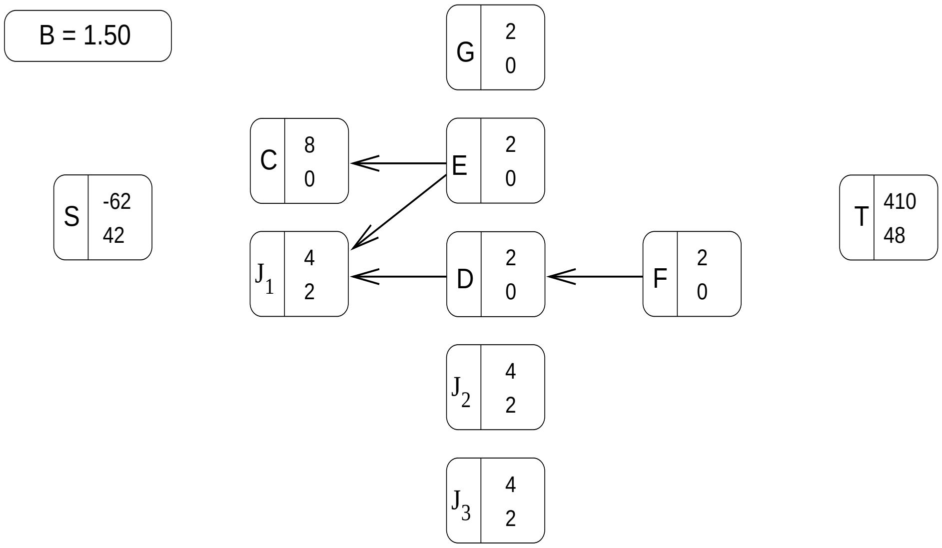

FIG. 5. Ground state $\overline{R}$ of sample DAFF ($L = 10$, $p = 0.5$) for $B = 1.5$.

At $B^j = 1.5$ a cluster J (an aggregation of the small clusters J_1, J_2, J_3) reverses its orientation. Here the number of total unsatisfied bonds is $N^u(9/7 < B < 1.5) = 39$ and $N^u(1.5 < B < 1.6) = 48$ (not visible from the graphic representation, but easily calculated using the spins from clusters S, T, because all other clusters have $N^u_C = N^s_C$). The magnetization of T changes from $m_T(B < B^j) = 42$ to $m_T(B > B^j) = 48$ (figure 6). Using formula (13) we get $B^j/J = \frac{|48-39|}{|48-42|} = \frac{9}{6} = 1.5$

Each of the clusters G, J_1, J_2 can take independently two orientations (=*states*). The clusters C, E alone can take three combinations of orientations because $s(E) = +1$ implies $s(C) = +1$. The clusters J_1, D, F alone can take 4 states. Because $s(E) = +1$ implies $s(J_1) = +1$ we have for all 5 clusters together $4 + 4 + (4 - 1) = 11$ states. So the system is $2^3x11 = 88$ fold degenerated.

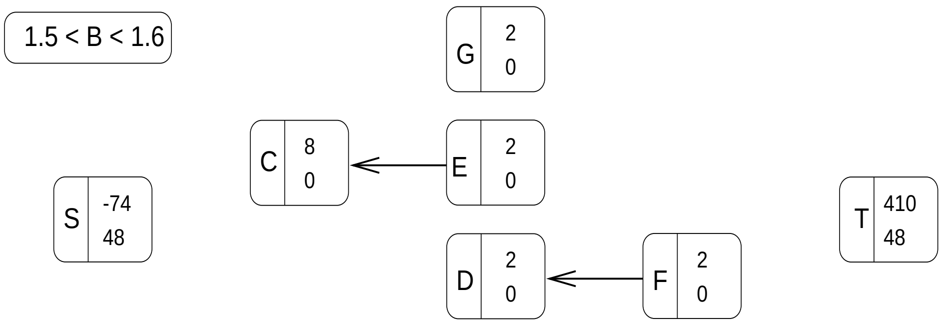

FIG. 6. Ground state $\overline{R}$ of sample DAFF ($L = 10$, $p = 0.5$) for $1.5 < B < 1.6$.

For $1.5 < B < 1.6$ the cluster J has been absorbed by the cluster S. Now the system has a degree of degeneracy of $2x3x3 = 18$. Note that the environment of the cluster J has changed during the jump as well. But only clusters V with $m_V = 0$ and $N^u_V = N^s_V$ are affected. So the formula for B^j/J is still correct.

Using the formulas (13, 16) the complete behavior of a DAFF/RFIM can be easily calculated. We show how the procedure works for a DAFF, the RFIM is similar. One starts with a certain value for $B = B_0$ (There must no jump occur, otherwise the formulas are not valid) and calculates the graph $\overline{R}(B_0)$. Then B is increased in macroscopic steps ΔB up to the value B_1 where the calculated graph $\overline{R}(B)$ differs from $\overline{R}(B_0)$ the first time. Then the jump-field B_i can be calculated from the graphs at B_0, B_1. One has to check if the jump is really the first jump occurring for $B > B_0$. This is done by calculating the graph $\overline{R}(B^j_-)$ for a field B^j_- which is infinitesimal smaller than B^j and comparing with $\overline{R}(B_0)$. If they are the same, the jump B^j is really the first for $B > B^j$. If not, a new jump-field $B^{j'}$ is calculated using $\overline{R}(B_0)$ and $\overline{R}(B^j_-)$ and at B^j may not be a jump at all. This procedure can be iterated until the jump next to B_0 is found.
It can be easily seen that this algorithm really produces the next jump starting from B_0. Suppose we have two jumps $B^j_1 < B^j_2$ between B_0 and B_1. Then B^j is given by (for a DAFF)

$$B^j/J = \frac{|N^u(B_0) - N^u(B_1)|}{|m_T(B_0) - m_T(B_1)|} \tag{17}$$

Because N^u and m_T are monotonic in B, the effect on that values of the both jumps sum up. So we have (B^j_+ slightly larger than B^j)

$$B^j/J = \frac{|N^u(B_0) - N^u(B^j_-)| + |N^u(B^j_+) - N^u(B_1)|}{|m_T(B_0) - m_T(B^j_-)| + |m_T(B^j_+) - m_T(B_1)|} \tag{18}$$

From $B^j_1 < B^j_2$ and because $n_1/d_1 < n_2/d_2$ implies $n_1/d_1 < (n_1 + n_2)/(d_1 + d_2) < n_2/d_2$ we get

$$B^j_1/J = \frac{|N^u(B_0) - N^u(B^j_-)|}{|m_T(B_0) - m_T(B^j_-)|} < B^j/J < \frac{|N^u(B^j_+) - N^u(B_1)|}{|m_T(B^j_+) - m_T(B_1)|} = B^j_2/J \tag{19}$$

By induction follows that the algorithm finds the next jump from B_0 for all number of jumps between B_0 and B_1. The next jump from a given jump B^j is found by restarting the algorithm at $B_0 := B^j_+$. Beside this linear search a bisection method starting with $B_0 = B_{start}$ and $B_1 = B_{end}$ should be possible. But we implemented the linear search, because it is more straight forward. Taking into account, that the calculation of the graphs $\overline{R}$ requires B, J to be integers, the linear search of all states $\overline{R}$ in a range $[B_{start}/J_0, B_{end}/J_0]$ can be algorithmically displayed as follows:

```
algorithm all ground states(B_start, B_end, J_0)
begin
    B ← B_start
    ΔB ← J_0
    stop ← false
    while ( not stop )
    begin
        B_0 ← B
        calculate R̄(B_0)
        same_R ← true
        while(same_R) /* Search for first state different from R̄(B_0) */
        begin
            if(same_R AND B > B_end) then
                stop ← true;
            else
            begin
                B ← B + ΔB
                calculate R̄(B)
                ΔB ← 2 * ΔB
                if( R̄(B_0) ≠ R̄(B)) then
                    same_R ← false
            end
        end
        if( stop) then
            continue
        found ← false
        B_1 ← B
        while( not found) /* search for next jump */
        begin
            B^j_- ← (int) [ |N^u(B_0) − N^u(B_1)| / |m_T(B_0) − m_T(B_1)| * J_0 + 0.5 ] − 1
            calculate R̄(B^j_-)
            if( R̄(B^j_-) = R̄(B_0)) begin
                found ← true
            else
                B_1 ← B^j_-
        end
        There is a jump at B^j ← |N^u(B_0) − N^u(B_1)|, J^j ← |m_T(B_0) − m_T(B_1)|
        B ← (int) [J_0 * B^j / J_j + 0.5] + 1
        ΔB ← difference between last two jumps
    end
end
```

Technical remarks:

- J_0 should be chosen sufficiently large. For the DAFF and the $\pm\Delta$-RFIM $J_0 > N$ guarantees to find all jumps. Since the values for b_i can take all real values for the Gaussian RFIM there is always a small probability of missing jumps. So we rounded the b_i-values to three significant digits and used $J_0 > 10^3 N$.
- The field increment ΔB used for searching the next state which is different from $\overline{R}(B_0)$ is set to the difference between the last two jumps found (initially J_0). During the search ΔB is doubled in each iteration, so jumps lying close to each other do not slow down the following calculations.
- The states $\overline{R}(B_0), \overline{R}(B_1), \overline{R}(B^j_-)$ must not be exactly at jumps in order to guarantees that the algorithm works. This is confirmed by checking if there are inner clusters with nonzero magnetization. If this is true the field B is in-/decrease about 1 up to a non-jump field (not shown in the algorithmic representation). For the DAFF/ $\pm\Delta$-RFIM this is guaranteed to be done in one step.
- For the DAFF/$\pm\Delta$-RFIM the states $\overline{R}$ at the jumps (B^j, J_j) can be calculated. For the Gaussian-RFIM that is not always possible directly, because the values of B_i are rounded off.

IV. RESULTS

We performed calculations of ground states over large B, Δ-intervals (values are related to $J = 1$) for system sizes $L = 8$ to $L = 48$ for the DAFF ($p = 0.5$), $\pm\Delta$-RFIM and the Gaussian-RFIM. The number of samples per system type and size are shown the table in figure IV.

L	DAFF $B \in [0,6]$	$\pm\Delta$-RFIM $\Delta \in [0,6]$	Gaussian-RFIM $\Delta \in [0,4]$
8	850	450	250
12	850	450	120
16	450	250	58
24	450	177	32
32	50	43	16
48	50	-	-

FIG. 7. Number of samples per system size and type.

For the $L = 48$ samples we reduced the B-interval to $[0.5, 1.5]$. For the $L = 32$ Gaussian-RFIM we reduced the Δ-interval to $[1.0, 2.8]$.
In figure 8 the antiferromagnetic order parameter per spin

$$a = \frac{1}{N} \sum_i \epsilon_i t(i) \sigma_i \tag{20}$$

of two DAFF systems with $L = 8$ and $L = 16$ over the whole range $B \in [0, 6.5]$ is displayed. Because of the ground state degeneracy many states are possible. Here the two extreme values, the order parameter can take, are shown. For the small system for $B < 1$ two states are possible, because its total magnetization is zero. The larger system has this feature only for $B < 0.5$. For both systems the range of possible a-values is relatively small for $1 < B < 2$ and little bit larger for $2 < B < 4$. The range is the largest for integer values I of B, because spins having neighbors with total magnetization I can take both orientations. The main differences between the two systems are: The larger system exhibits more jumps and the order parameter decreases more quicker than for $L = 8$.
The discrete structure is clearly visible. In both systems the order parameter is high for small fields and goes stepwise to zero.

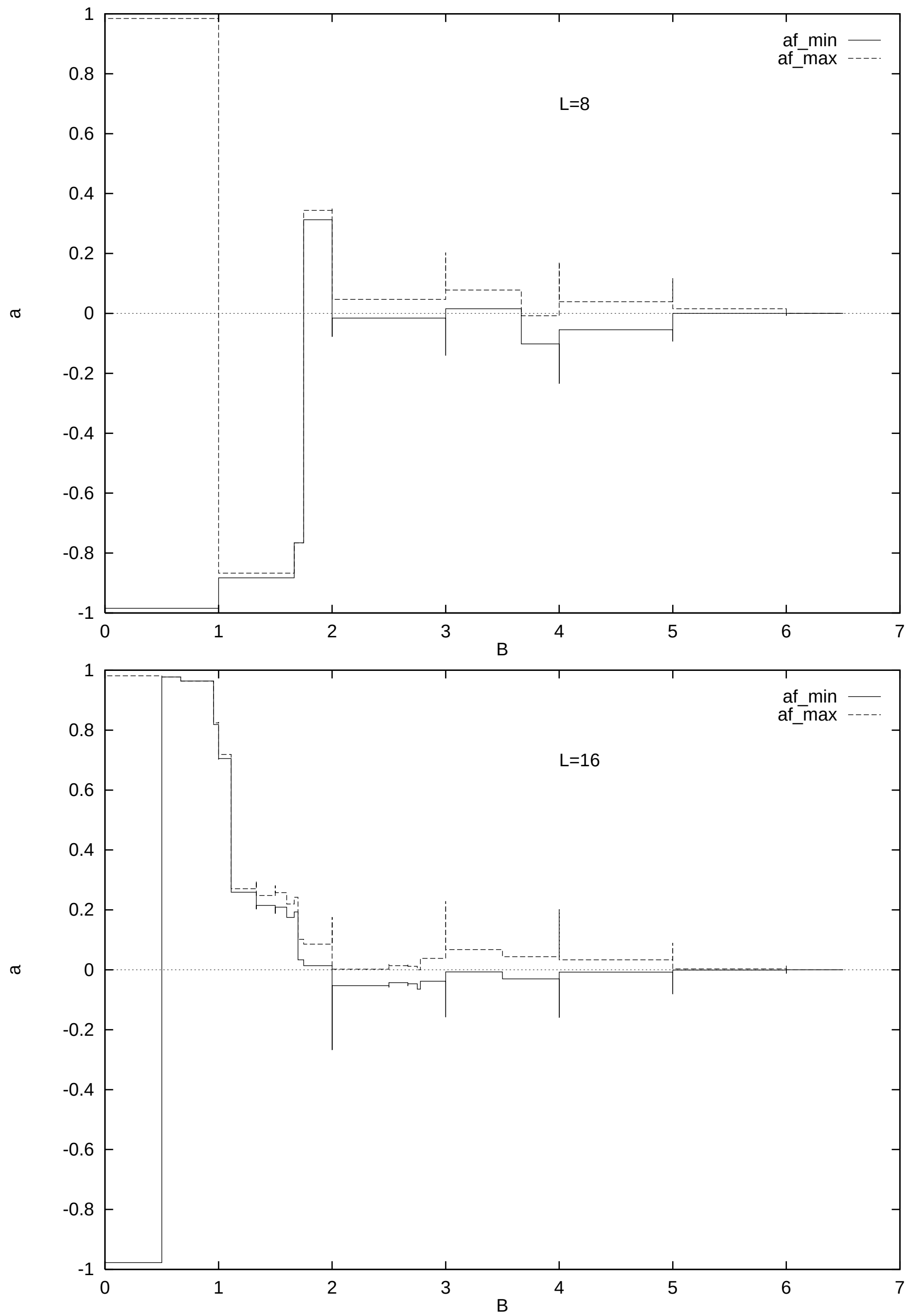

FIG. 8. Antiferromagnetic order parameter of sample DAFFs ($L = 8$, $p = 0.5$) and ($L = 16$, $p = 0.5$.) for $0 \leq B < 6.5$.

Because of the step-structure it is difficult to obtain 'critical' magnetic fields by calculation of susceptibilities and then use finite size scaling to go to the $L \to \infty$ limit. Instead we proceed as follows, to get first informations about how the order parameter changes. We calculated for each sample the *barrier field value* $B_{a<a_0}$ where the order parameter a falls the first time below a_0, i.e.

$$B_{a<a_0} = \min\{B|a(B) < a_0\} \tag{21}$$

In figure 9 the average $B_{a<a_0}$ is plotted against the inverse system size $1/L$ for $a_0 = 0.2, 0.5, 0.8$. Just to get a first impression we extrapolated to $L \to \infty$ by fitting straight lines $B_{a<a_0}(1/L) = c/L + B_{a<a_0}(0)$. The fit seems to be good, but may have no physical meaning. From the figure we can see that $B_{a<0.5}(0) = 0.90 \pm 0.02$, so the transition to the domain state occurs for $B_c < 1$! This is in contradiction to previous results from MC calculations of systems of size 60x60x61 [5] where $B_c \approx 1.4$ was found. Because we want to rule out the influence of the fit function, we checked the result by calculating the ground states for ten $L = 160$ systems, at $B = 0.9999$ where we got an average order parameters of 0.22 ± 0.11. So the infinite system has no long range order for $B > 0.9$! From figure 9 we can't see, whether the $[B_{a<0.8}, B_{a<0.2}]$ interval remains finite or becomes infinitely small for the $L = \infty$ system. More calculations and larger systems are needed.

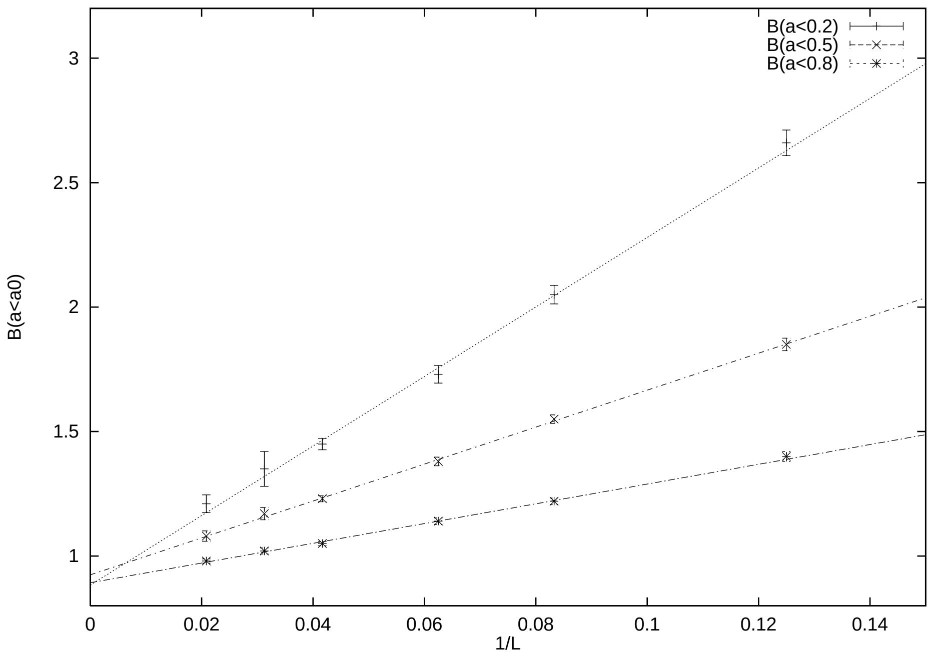

FIG. 9. Barrier field $B_{a<a_0}(1/L)$ for $L = 8, \ldots, 48$ ($a_0 = 0.2, 0.5, 0.8$) and fit functions $B_{a<a_0}(1/L) = c/L + B_{a<a_0}(0)$.

In figure 10 diagrams are shown for the magnetization per spin

$$m = \frac{1}{N} \sum_i \sigma_i \tag{22}$$

of two sample $\pm\Delta$-RFIM.

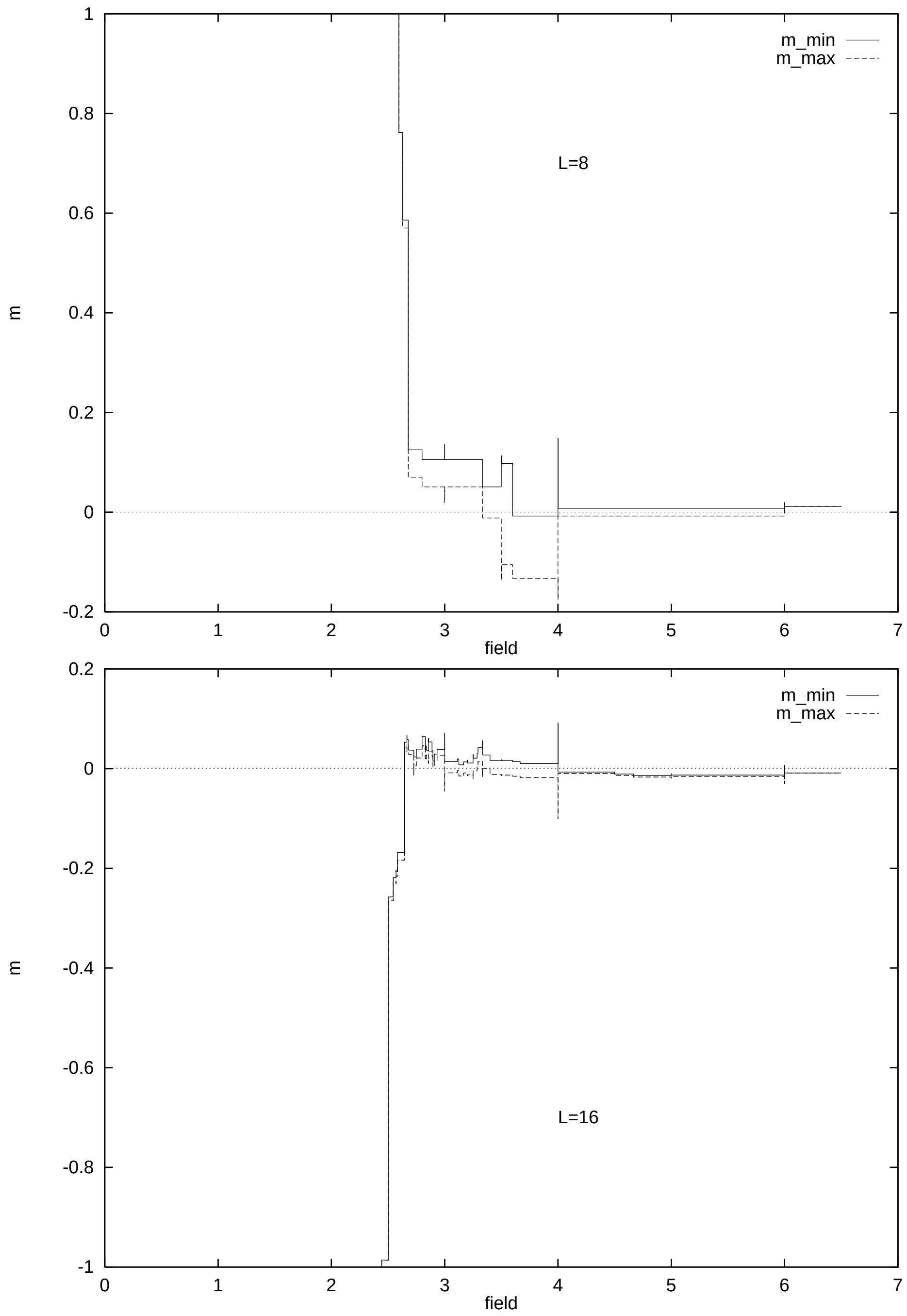

FIG. 10. Antiferromagnetic order parameter of sample RFIMs ($L = 8$) and ($L = 16$) for $0 \leq \Delta < 6.5$.

The impression is similar to the DAFF, but the order parameter goes to zero at higher fields and there are more jumps in the system because there are more spins in a RFIM than in a DAFF of the same size L. Diagrams of Gaussian-RFIM look similar but there are even more jumps in a system of equal size and the decrease of the order parameter is less rapid.
In analogy to the DAFF we calculated the barrier fields $\Delta_{m<m_0}$ for the random field systems. They are display in figure 11

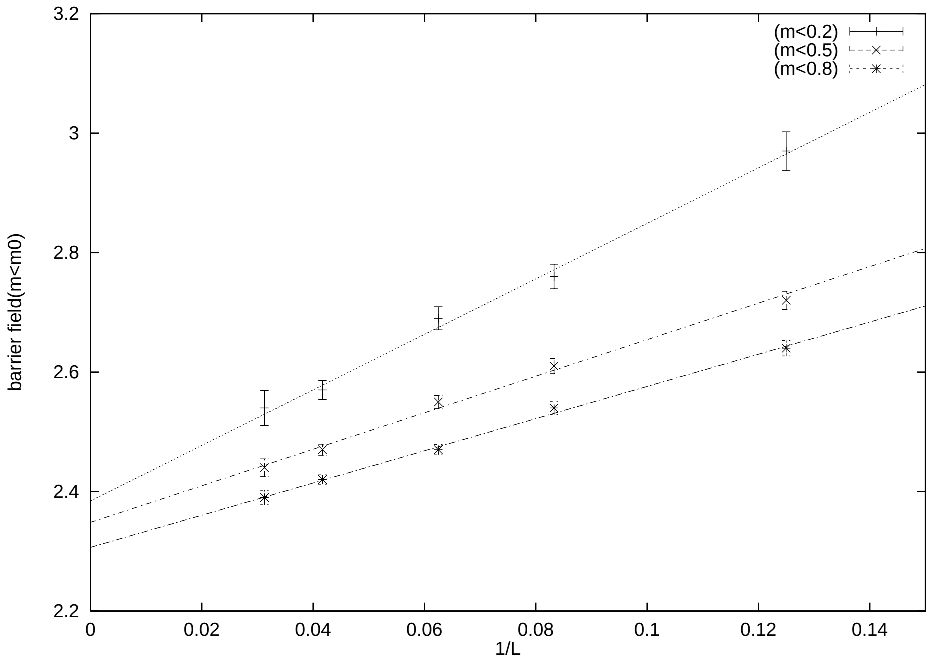

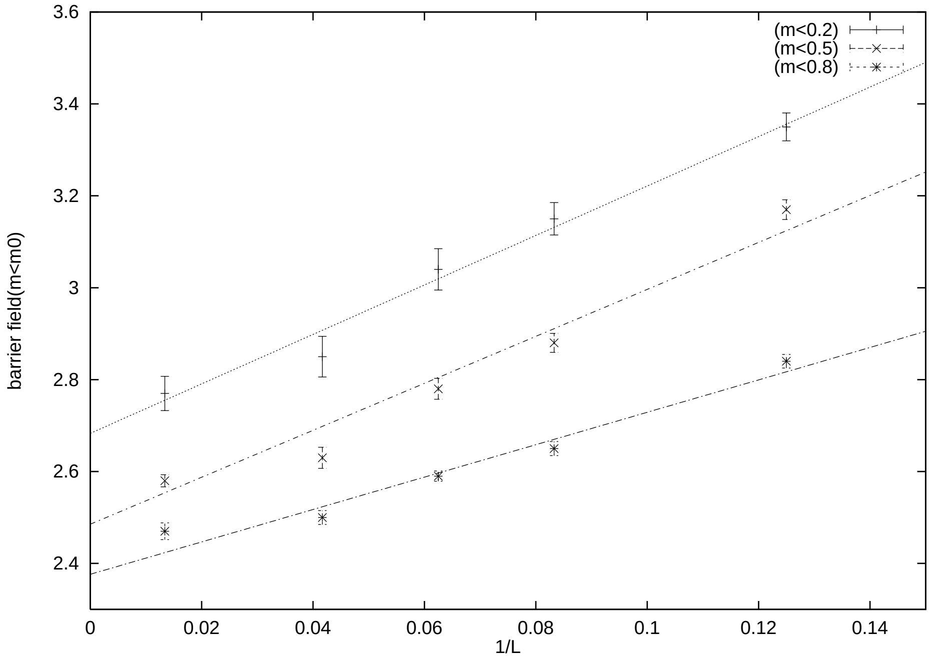

FIG. 11. Barrier field $\Delta_{m<m_0}(1/L)$ for $L = 8, \ldots, 32$ ($m_0 = 0.2, 0.5, 0.8$) and fit functions $\Delta_{m<m_0}(1/L) = c/L + \Delta_{m<m_0}(0)$.

We got the values $\Delta_{m<0.5}(0) = 2.35 \pm 0.01$ ($\pm\Delta$) and $\Delta_{m<0.5}(0) = 2.49 \pm 0.04$ (Gaussian) for the infinite systems. The value for the $\pm\Delta$ system is consistent with previous calculations [8].

For the Gaussian-RFIM the values are less reliable, because we could calculate only few systems. The Gaussian systems exhibit many jumps and the number of ground states which have to be calculated is about six times the number of jumps. So many ground states have to be calculate to analyze the system, resulting in more computer time needed.

For all types of systems the number of jumps $\#j$ increases with system size. Figure 12 shows this dependence. The number of jumps increases roughly like $\#j(L) = c * L^b$ with $b = 1.23 \pm 0.04$ (DAFF), $b = 1.76 \pm 0.01$ ($\pm\Delta$-RFIM), $b = 2.91 \pm 0.03$ (Gaussian-RFIM, only jumps in $\Delta \in [1.0, 2.8]$ are counted, the number of jumps in [0.0,6.0] is about four times higher !) This means that the behavior of the system gets smoother with increasing size, i.e. the infinite system looses the discrete structure on finite B, Δ-scales.

We measured also the number of jumps in the B, Δ-interval where the order parameter falls from 0.8 to 0.2 for each system. Even this number increases although the interval is reduced with increasing system size. We performed a similar fit to the case above and obtained $b = 0.90 \pm 0.02$ (DAFF), $b = 1.40 \pm 0.06$ ($\pm\Delta$-RFIM) and $b = 2.18 \pm 0.02$ (Gaussian-RFIM).

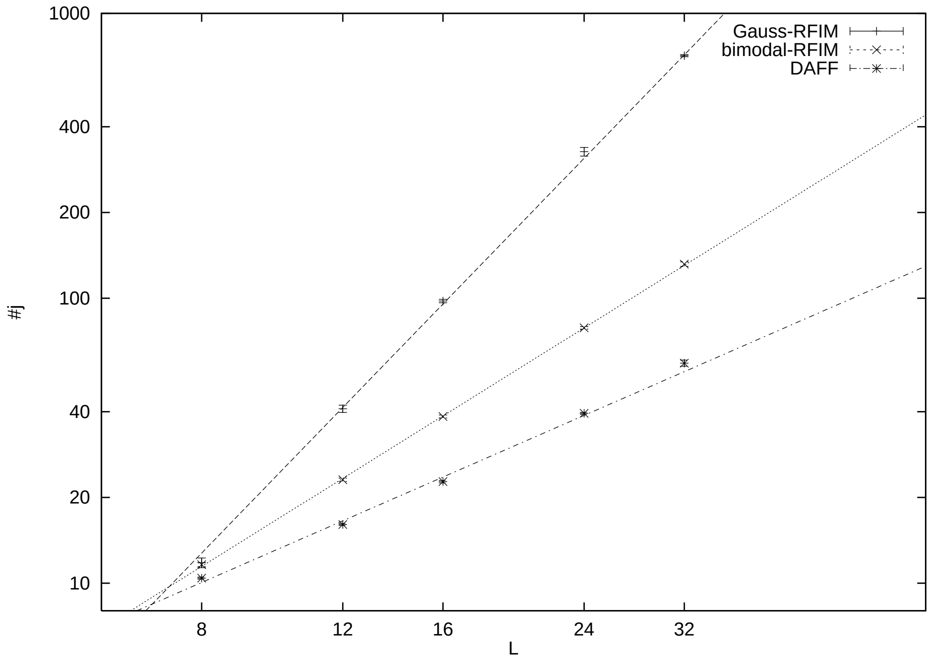

FIG. 12. Average number of jumps in $B \in [1, 2.8]$ (Gaussian-RFIM) resp. $[0, 6]$ ($\pm\Delta$-RFIM, DAFF) as function of system size in a double logarithmic scale and fit functions $\#j(L) = cL^b$.

In the last part we focus on the degree of degeneracy (dod). In figure 13 the dod of the sample DAFF systems is displayed as function of the field B. The dod is not calculated exactly, but estimated very accurately[2] by an algorithm found in [18].

---

[2]For the graph types which occur here, the estimate seems to be exact: For small systems the value is the same. For large system the type of the graph is the same, as we will see.

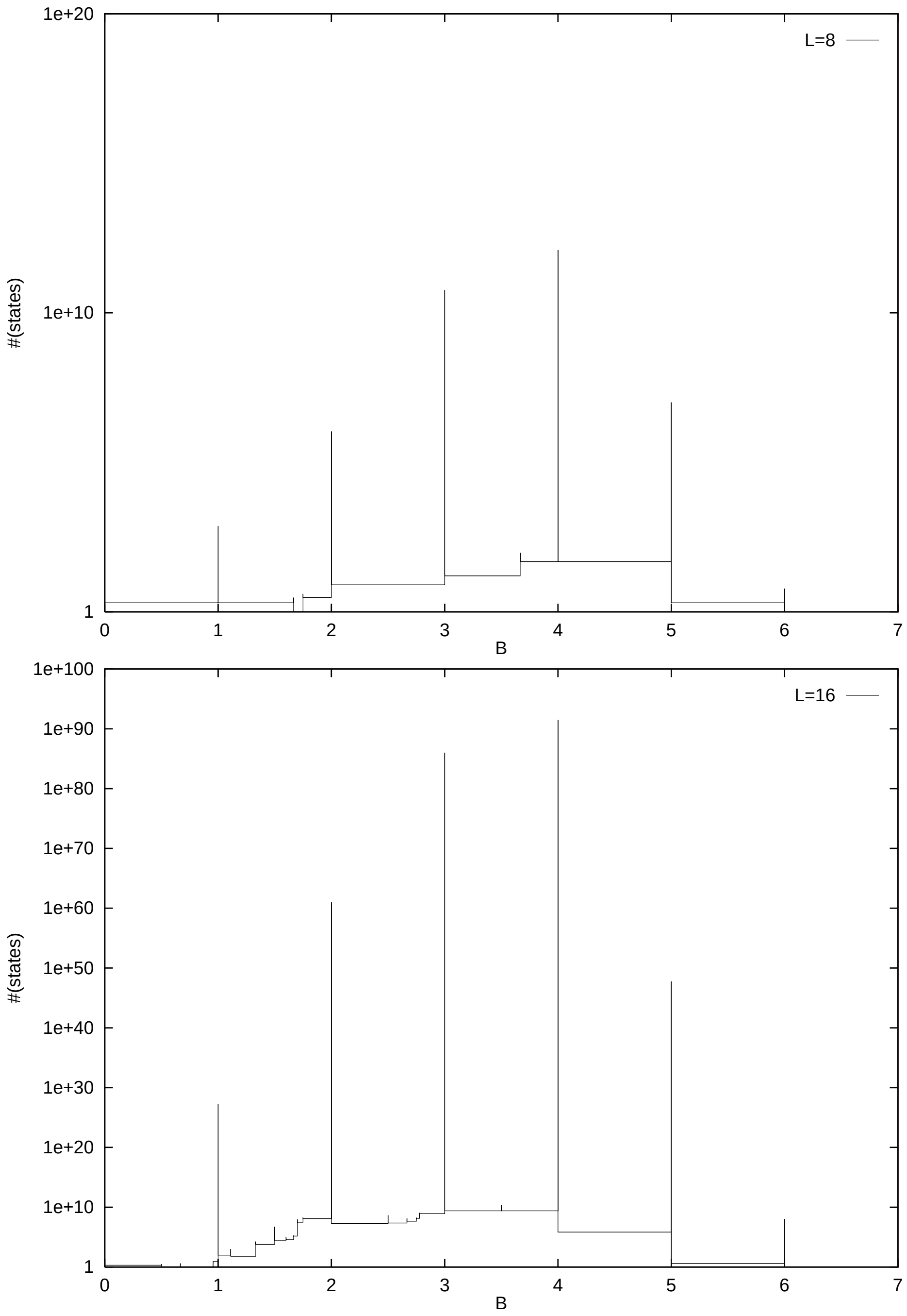

FIG. 13. Degree of degeneracy of sample DAFFs ($L = 8$, $p = 0.5$) and ($L = 16$, $p = 0.5$) for $0 \leq B < 6.5$.

The degree of degeneracy is there very large, where the external field takes integer values. For non integer values the dod takes the largest values for $B \in (3, 4)$.
We found that there are only small connected subgraphs in $\overline{R}$ of small height (the maximum length path in the graph) at fields B where no jump occurs. So the spin-clusters contributing to the degeneracy are flipping almost independently, i.e. the ground state structure is quite simple. That means that the number of states are not reduced very much from $2^{\#n}$, where $\#n$ is the number of inner clusters.
We could find that the average dod can be approximated very good by a function of $\#n$ and of the number of edges $\#e$ in $\overline{R}$ over the full B-range:

$$\mathrm{dod} = 2^{\#n}\alpha^{\#e} \tag{23}$$

This means, that for $\#e = 0$ all inner clusters are independent, so the dod depends exponential on the number of nodes. The edges put constraints on the nodes, so the number of possible states is reduced. So it is possible to describe the ground state structure by a single value α. We measured $\alpha \approx 0.79 \pm 0.03$. This value is quite independent of the system size and the external field[3].

[3]The distribution of α-values has a peak at $\alpha = 0.75$. That is the value of a system consisting only of independent clusters and of pairs of clusters each connected by one edge.

Figure 14 shows the dod for the two sample $\pm\Delta$-RFIM systems. Here the dod takes its largest values at the integer-fields $\Delta = 3, 4, 6$ and in $(3, 4)$. For the Gaussian-RFIM *no degeneracy* occurs except the twofold degeneracy at the jumps. This is to be expected, because it is very unlikely that the sum of the random fields Σ_C is zero for a cluster C. The dod of the $\pm\Delta$-RFIM can also be approximated very well by equation (23). We got an average $\alpha = 0.7582 \pm 0.0002$.

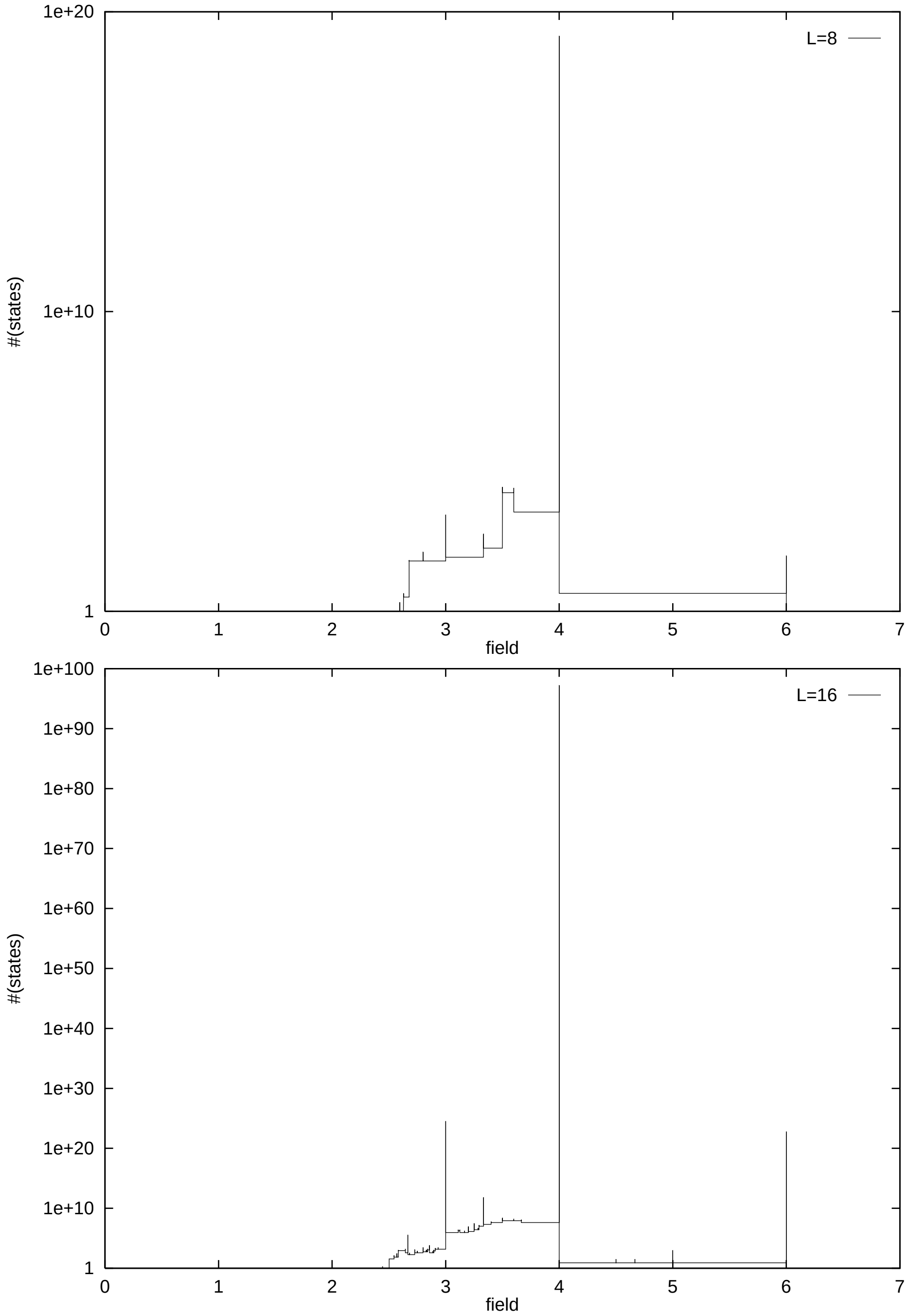

FIG. 14. Degree of degeneracy of sample RFIMs ($L = 8$) and ($L = 16$) for $0 \leq \Delta < 6.5$.

Since the dod is mainly determined by the number $\#n$ of (inner) clusters and the number $\#e$ of edges, we calculated these values for the DAFF/$\pm\Delta$-RFIM at $B = \Delta = 3.9999$ for sizes up to $L = 160$ (from 2560 realizations for $L = 12$ to 10 realizations for the largest systems). The result is shown in figure 15.

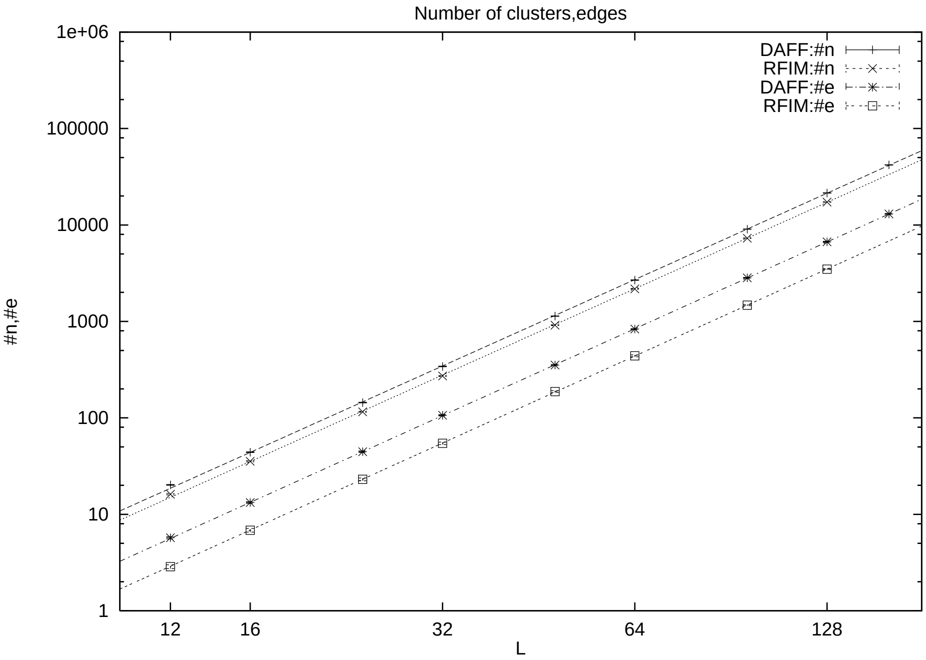

FIG. 15. Number of clusters $\#n$, edges $\#e$ as function of system size L for the DAFF and the $\pm\Delta$-RFIM together with fits of form $f(L) = cL^b$.

For both system types all numbers have a $L^{3.00}$ dependence on L. The number of edges is about 3 to four times smaller than the number of clusters. For the DAFF about 4.6 percent of the spins are contained in the inner clusters, for the $\pm\Delta$-RFIM this value is only 1.8 percent. These values are almost independent of the system size. Because the number of clusters/state depend linearly on the system size, this shows again that the ground state of the DAFF/RFIM consist of many independent small clusters. So the number of clusters increases, but not the size of the clusters and not the degree of connection between the clusters. This means that the degree of degeneracy depends exponential on the size of the system.

V. CONCLUSIONS

In this paper we have presented an algorithm for calculating exact ground states of random field systems and diluted antiferromagnets in polynomial time for all fields B, Δ. The complete degeneracy of all states is representable by a relation of (anti-)ferromagnetic clusters. The use of new fast algorithm allowed us to calculate systems of sizes up to 160^3.
We found that the transition to the domain states occurs for the DAFF at $B_c < 1$ in contradiction to previous results. The result for the $\pm\Delta$-RFIM $\Delta_c = 2.35 \pm 0.01$ was consistent with previous calculations. For the Gaussian RFIM we found $\Delta_c = 2.49 \pm 0.04$.
The order parameters of the systems are stepwise constant functions of the field. The number of jumps inside a given B, Δ interval increases faster than L, indicating that the infinite system has a rather smooth behavior.
The ground state degeneracy of the DAFF and the $\pm\Delta$-RFIM is very high, especially when the field is integer valued. Apart from these values the degree of degeneracy is at highest in the domain state. The degree of degeneracy increases exponentially with system size. The degeneracy is rather simple, because the ground states consist of many small, only loosely coupled clusters. Not more than 5 resp. 2 percent of all spins contribute to the degeneracy. The Gaussian-RFIM is not degenerated at all, except at the jump fields, where one cluster can take two orientations.
Using the methods presented and referenced in this paper many more information about the ground state structure of DAFFs and RFIMs will be obtained in the future. A detailed analysis of the numbers, sizes and forms of the clusters forming the ground states and type of connections between them is possible. Because the systems get smoother with increasing size, finite size scaling techniques should be applicable, to gain more insight into the transition from the long range order to the domain state.

VI. ACKNOWLEDGMENTS

We would like to thank D.W. Heermann for manifold support and K.D. Usadel and J. Esser for fruitful discussions and critical reading of the manuscript. We thank the *Paderborn Center for Parallel Computing*, the *Universitäts-rechenzentrum Heidelberg* and the *Rechenzentrum Universität Duisburg* for the allocation of computer time. This work was supported by the Graduiertenkolleg “Modellierung und Wissenschaftliches Rechnen in Mathematik und Naturwissenschaften” at the *Interdisziplinäres Zentrum für Wissenschaftliches Rechnen* in Heidelberg.

[1] K. Binder and A.P. Young, Rev.Mod.Phys. 58 (1986), 801
D.P. Belanger and A.P. Young, JMMM 100 (1991), 272
[2] S. Fishman and A. Aharony, J.Phys C 12 (1979), L729
[3] J.L. Cardy, Phys.Rev. B 29 (1984), 505
[4] J.A. Cambier and M. Nauenberg, Phys.Rev. B 34 (1986), 7998
[5] U. Nowak and K.D. Usadel, Phys.Rev. B 44,14 (1991), 44
[6] U. Nowak and K.D. Usadel, Phys.Rev. B 46 (1992), 8329
[7] J. Esser, U. Nowak, K.D. Usadel, Phys.Rev.B 55 (1997), 5866
[8] A.T. Ogielski, Phys.Rev.Lett 57 (1986), 1251
[9] A.K. Hartmann and K.D. Usadel, Physica A 214 (1995), 141.
[10] J.L. Träff, Eur.J.Oper.Res. 89 (1996) 564.
[11] J.-C. Picard and M. Queyranne, Math.Prog.Study 13 (1980), 8.
[12] K.D. Usadel and U. Nowak, JMMM 104-107 (1992), 179
[13] M.N.S. Swamy and K. Thulasiraman, Graphs, Networks and Algorithms (Wiley, New York 1991).
[14] J.D. Claiborne, Mathematical Preliminaries for Computer Networking (Wiley, New York, 1990).
[15] W. Knödel, Graphentheoretische Methoden und ihre Anwendung (Springer, Berlin, 1969)
[16] J.-C. Picard and H.D. Ratliff, Networks 5 (1975), 357.
[17] R.E. Tarjan, Data Structures and Network Algorithms (Society for industrial and applied mathematics, Philadelphia 1983).
[18] L. Schrage, K.R. Baker, Oper.Res. 26,3 (1978), 444.